Thermal Analysis of Wall/Floor Intersections in Building Envelope

Pyeongchan Ihm†

Joint Center for Energy Management, CEAE Department, CB 428,
University of Colorado, Boulder, CO 80309, USA

Key words: Thermal bridge, Finite difference method, Heat transfer

ABSTRACT: Wall/floor intersection is important parts of a building envelope system. These intersections can be sources of thermal bridging effects and/or moisture condensation problems. This paper provides a detailed analysis of the thermal performance of wall/floor intersection. In particular, two-dimensional steady-state and transient solutions of the heat conduction within the wall/floor joint are presented. Various insulation configurations are considered to determine the magnitude of heat transfer increase due to wall/floor joint construction.

Nomenclature

C_p : specific heat [Btu/lb.°F]
h : connective heat transfer coefficient
k : thermal conductivity [Btu/hr.ft.°F]
r : vector space of x, y
t : time [hour]
T : ambient temperature [°F]
T_{ss} : wall and slab surface temperature [°F]

Greek symbol

ρ : density of material [lb/ft^3]

1. Introduction

In current energy analysis procedures, the building envelope components are analyzed separately. However, most of these components are integrated together. Building envelope component intersections are prone to thermal bridging effects such increase of heat transfer and/or moisture condensation problems. Therefore, special care should be considered in the thermal analysis of wall/floor intersection.

To perform an energy analysis of a building envelope, it is a common practice to assume that for each component (such as walls, floor, or roof) heat follows a one-dimensional path. However, this is not always the case, especially at sections of the building envelope where walls meet with the floor or the roof. Indeed, at the wall/floor joint, the heat conduction has at least a two-dimensional character typically resulting in higher heat losses and lower interior surface temperature than would be predicted by one-dimensional analysis methods. When interior envelope surface temperature drops below the dew point of the surrounding air inside the building, moisture condensation may occur and structure damages may result.

Two-dimensional analysis of various building envelope sections has been developed by a number of authors including Carslaw and Jaeger,[1] Langmuir et al.,[2] Letherman and Sarkis,[3] Mathews.[4] Most of the available studies assume isothermal boundary conditions for both outside and inside envelope surfaces to arrive at an analytical or graphical solution of the heat conduction equations. These solutions are

† Corresponding author
Tel.: +1-303-492-0516; fax: +1-303-492-7317
E-mail address: ihmp@colorado.edu

typically used to calculate conduction shape factors. Recently, Mao and Johannesson,[5] Kim et al.,[6] Al-Sanea[7] and Fukuyo[8] developed analytical or numerical model to analyze the thermal bridge effect of building envelope. However, a detailed analysis of wall/floor joint is limited when both steady-state and transient conditions are considered.

Two spaces with different indoor room temperatures such a conditioned house above a crawlspace or an unheated basement are considered. The analysis of this room configuration provides the effects of insulation levels and the heat transfer to both outdoor environment and unconditioned spaces and suggests the optimal insulation installation to minimize heat loss and to prevent moisture condensation of the conditioned room from unheated space.

This paper provides a summary of the results of a detailed study to investigate the thermal performance of several insulation configurations for wall/floor intersection. The first section describes briefly the numerical solution used to solve the heat conduction within the various elements of the building envelope. The second section of this paper presents a compilation of some of the results obtained by the numerical solution to characterize the temperature distribution, the surface heat flux, and the total heat transfer for a wall/floor joint that separates two spaces with different indoor air temperatures.

2. Solution approach

2.1 Problem description

Figure 1 illustrates a model for an exterior wall and a floor separating a conditioned room and an unconditioned space such as a crawl space. The unconditioned space air temperature depends on both the outdoor ambient and indoor room temperatures. Thermal insulation can be placed either at the inside or the outside

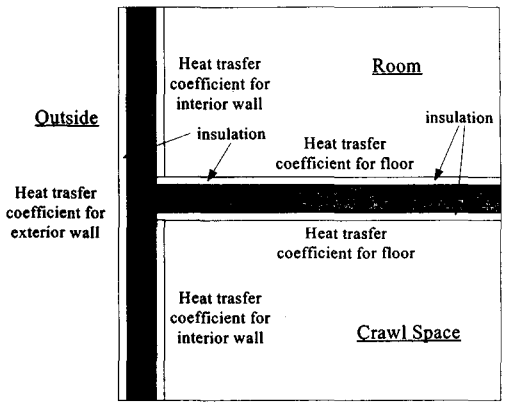

Fig. 1 Model of a crawl space structure.

wall/floor surfaces. The problem is to determine the effect of the insulation placement on the thermal performance of both the wall and the floor.

2.2 Mathematical formulation

The temperature field within the building envelope is subject to the time-dependent heat conduction equation in a non- isotropic medium and can be expressed by the following differential equation:

$$\frac{\partial}{\partial x}\left\{k\frac{\partial T(r,t)}{\partial x}\right\}+\frac{\partial}{\partial y}\left\{k\frac{\partial T(r,t)}{\partial y}\right\} = \rho c_p \frac{\partial T(r,t)}{\partial t} \quad (1)$$

For steady-state conditions, the temperature field of the building envelope is solution of the following equation:

$$\frac{\partial}{\partial x}\left\{k\frac{\partial T(r,t)}{\partial x}\right\}+\frac{\partial}{\partial y}\left\{k\frac{\partial T(r,t)}{\partial y}\right\} = 0 \quad (2)$$

The interior and exterior wall surfaces and slab interior surface can be modeled by a convective type boundary condition. Specifically, the heat flux to or from the wall and the floor surfaces is governed by Newton's equation:

$$q = h_\infty (T_\infty - T_{ss}) \quad (3)$$

2.3 Finite difference solution

Using a pure implicit finite difference technique (Pantankar[9]), Eq. (1) can be solved. The pure implicit method was chosen since it provides a solution that is unconditionally stable. Indeed, an implicit finite difference solution has the advantage of providing a stable solution for any space and time increment. That is, there is no stability criterion nor any restriction on the selection of space or time increment.

The control volume and its associated nodal dimensions are shown in Fig. 2. For a node P, E and W are its x-direction neighbors, while N and S are its y-direction neighbors. The shaded area shows the control volume of node P. Thus, Eq. (1) can be discretized as follows:

$$a_p T_p = a_E T_E + a_W T_W + a_N T_N + a_S T_S \quad (4)$$

where,
$$a_E = k_E \Delta Y/(\delta x)_E$$
$$a_W = k_W \Delta Y/(\delta x)_W$$
$$a_N = k_N \Delta X/(\delta x)_N$$
$$a_S = k_S \Delta X/(\delta x)_S$$

with,
$$a_p^0 = \frac{\rho C_p \Delta x \Delta y}{\Delta t}$$

The steady-state heat conduction solution (i.e., solution for Eq. (2)) can be easily obtained from the transient solution by setting the specific heat (C_p) to zero.

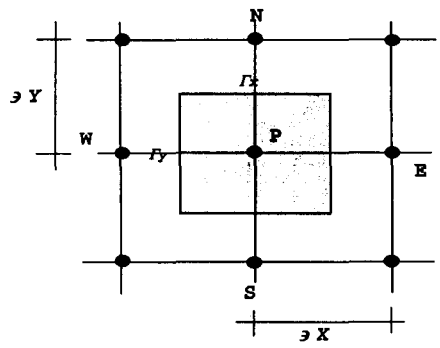

Fig. 2 Control volume for the two-dimensional heat conduction problem.

Once the nodal network is set and an appropriate finite difference equation is written for each node, a system of linear algebraic equations is obtained and needs to be solved. Standard or general matrix solvers such as Gauss-Jordan and Gauss-Seidel methods are not suitable for this relatively large set of equations. Instead, a special matrix solver called "LAPACK[10]" is used to solve the set of linear systems.

2.4 Discretization of building structure

Typically, the discretization grid is selected to be fine near surface boundary conditions and near the interface between any two materials with different thermal properties and is rough in the middle of the domain (i.e., wall or floor layers). This non-uniform discretization scheme is usually used to save computer time. For this study, a uniform but fine discretization is used to obtain accurate solution. The space increments used are x=0.0467 ft (1.4 cm), and y=0.05 ft (1.5 cm). The total nodal points are 8500 for the model of wall/floor intersection presented in Fig. 2.

Two approaches are used to model the effect of the thermal insulation. The first approach models the actual thickness of the insulation layer. In the second approach, the insulation layer thickness is neglected but its thermal resistance (i.e., R-value) is included in the heat transfer coefficient at wall or floor.

2.5 Analysis parameters

Figure 3 presents six insulation placements for both wall and floor surfaces when the wall/floor intersection separates a conditioned space from an unconditioned area. For this study, three insulation levels are used R-5 (1.03 $m^2 \cdot ℃/W$), R-10 (2.05 $m^2 \cdot ℃/W$), and R-20 (4.10 $m^2 \cdot ℃/W$). In addition, thermal conductivity values of

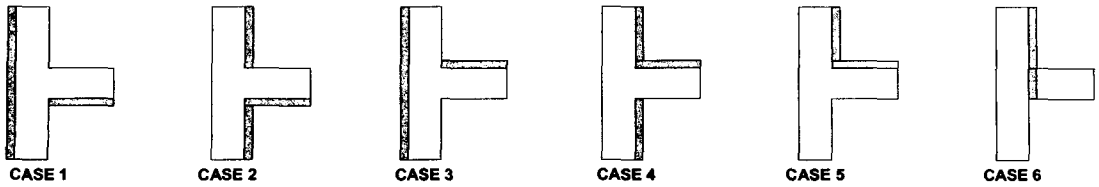

Fig. 3 Insulation location for the crawl space structure.

these insulation levels are 0.97 kcal/m^2·h·℃, 0.49 kcal/m^2·h·℃, 0.24 kcal/m^2·h·℃, respectively. For example, R-10 can be used to comply Korean thermal conductivity level of exterior wall as 0.5 kcal/m^2·h·℃ applying Southern region.

3. Results and discussion

3.1 Steady state results

Figure 4 shows the temperature isotherms within the wall/floor joint when R-10 (2.05 m^2·℃/W) thermal insulation is placed (i) at the outside of the wall surface and (ii) at the lower surface of the floor (i.e., case 1 as shown in Fig. 3). The conditioned room air temperature is kept at 70°F (21.1℃), while the outdoor air temperature is −12°F (−11.1℃) [winter conditions], and the unconditioned space air temperature is 27.8°F (−1.8℃). Both the walls and the floor are made up of concrete. Figure 4(a) presents the temperature within the wall/floor intersection for the case where the thermal insulation is modeled by a heat transfer coefficient. Figure 4(b) illustrates the temperature isotherms for the case where the actual layer of the thermal insulation is modeled.

Figures 4(a) and 4(b) indicate almost the same temperature pattern within the concrete layer of both the wall and the floor. However, the temperature changes significantly within the insulation layer when it is accounted for as shown in Fig. 4(b). Both Figs. 4(a) and 4(b) clearly illustrate the two-dimensional nature of

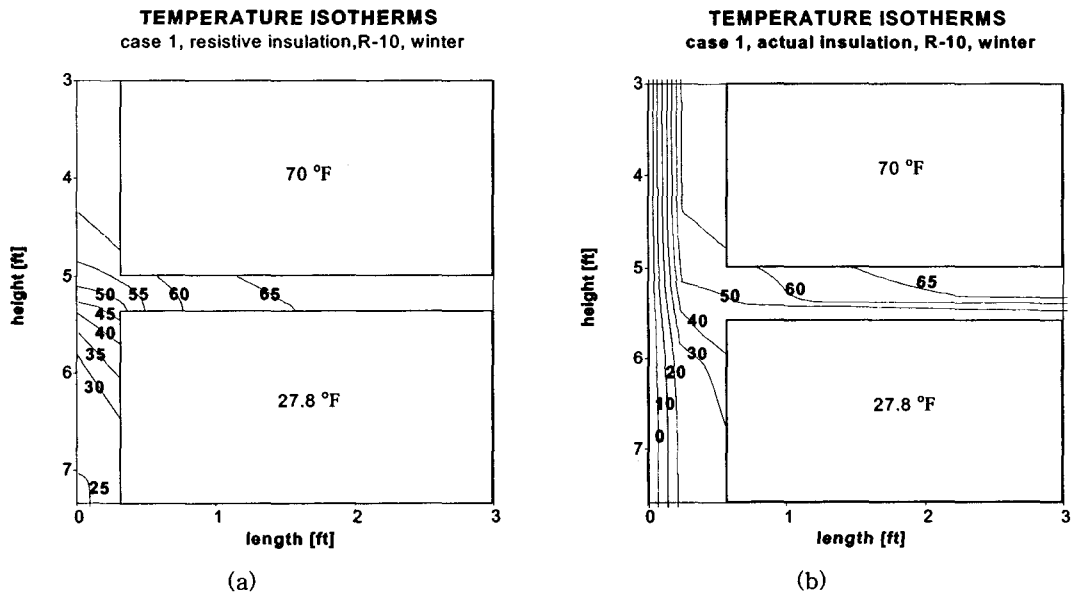

(a) (b)

Fig. 4 Temperature isotherms for the insulation configuration of case 1 (Conversion: [°F-32]×5/9=℃, 1 ft=0.3 m).

the temperature variation in the neighborhood of the wall/floor joint. Later on in this paper, the increase in heat transfer due to the wall/floor joint will be discussed in detail.

Figure 5 presents the temperature distribution within the wall and the floor when thermal insulation is placed at the inner wall surface and at the top of the floor surface as indicated for case 4 in Fig. 3. For Fig. 5, the insulation layer is modeled as a resistive coefficient (included in the heat transfer coefficient at the inner surface of both the wall and the floor) with no physical thickness. The indoor air temperature is kept at 70°F (21.1℃), while the outdoor ambient air temperature is −12°F (−11.1℃). The unconditioned space air temperature is allowed to float and depends on the insulation thermal resistance. The temperature distribution within the wall/floor intersection changes with the thermal resistance of the insulation as shown in Fig. 5(a) for R-5 (1.03 $m^2 \cdot ℃/W$) insulation, in Fig. 5(b) for R-10 (2.05 $m^2 \cdot ℃/W$) insulation, and in Fig. 5(c) for R-20 (4.10 $m^2 \cdot ℃/W$) insulation.

Figure 5 shows that the higher the thermal insulation R-value, the colder the floor and the wall interior surfaces. It is because the thermal insulation layer is modeled by a simple coefficient. Generally, the higher the thermal insulation R-value, the closer to the room air temperature the floor and the wall interior sur-

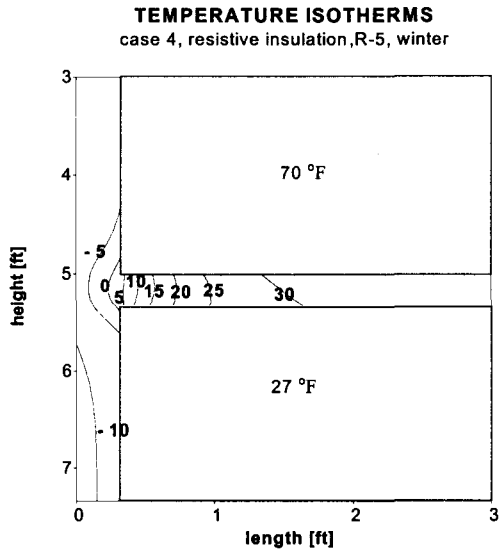

(a)

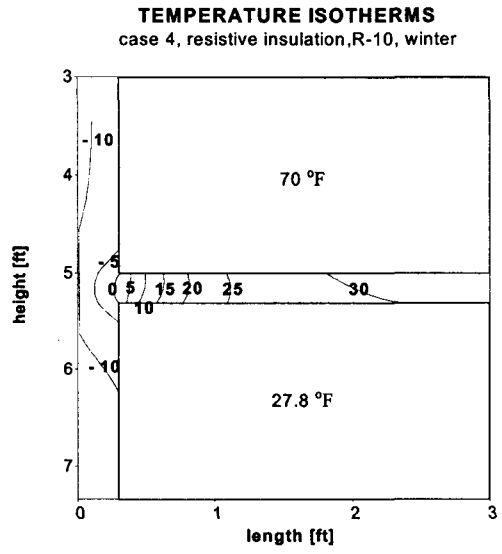

(b)

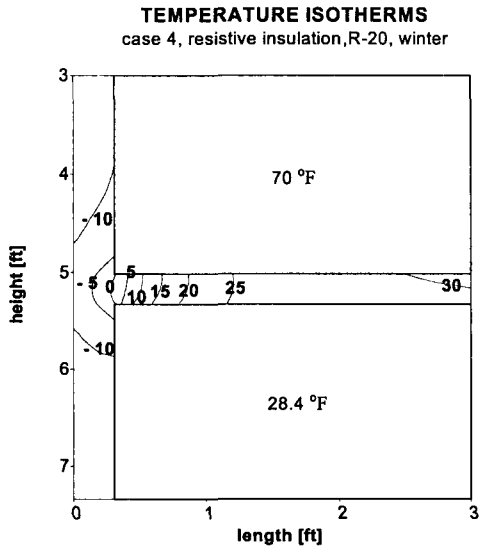

(c)

Fig. 5 Temperature isotherms for the insulation configuration of case 4 (Conversion: [°F-32]×5/9=℃, 1 ft=0.3 m).

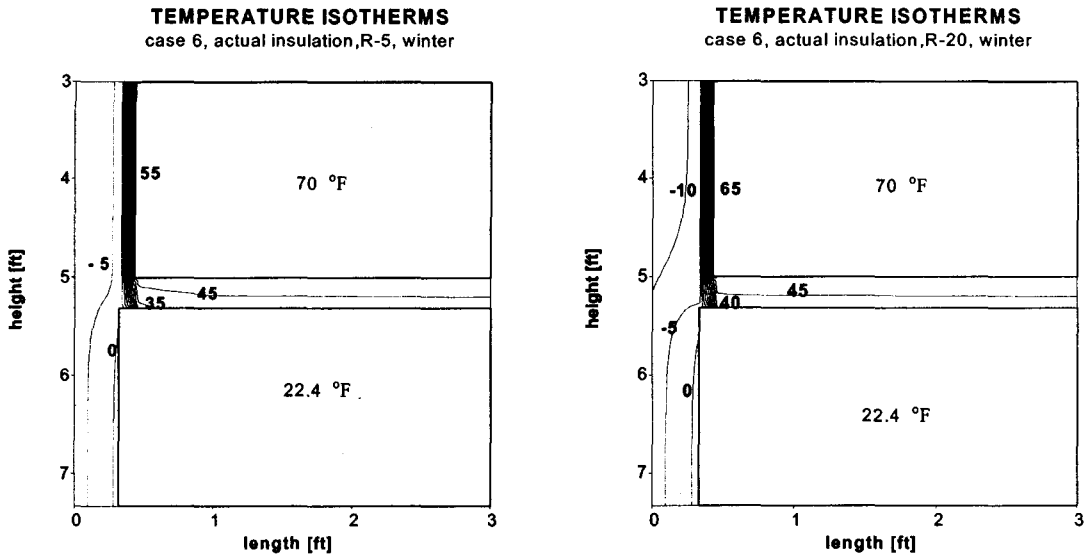

(a) (b)

Fig. 6 Temperature isotherms for the insulation configuration of case 6 (Conversion: [°F-32]×5/9=℃, 1 ft=0.3 m).

face temperatures. In addition, Fig. 5 indicates that the temperature gradient is high at the joint section connecting the floor to the wall. This result indicates that a large heat transfer loss occurs at the wall/floor joint. This significant temperature gradient at the joint section is independent of the level of thermal insulation.

Figure 6 shows the temperature distribution for the insulation configuration presented by case 6 in Fig. 3 (i.e., the thermal insulation layer is placed only at the inner wall surface of the conditioned space but extends to the wall/floor joint). Two insulation levels are considered: R-5(1.03 m^2·℃/W) in Fig. 6(a) and R-20 (4.10 m^2·℃/W) in Fig. 6(b). The air temperature is 70°F (21.1℃) in the conditioned space, and is 22.4°F (−5.3℃) in the unconditioned space. The actual thickness of the insulation is modeled to obtain the results shown in Fig. 6. The higher insulation level results in an increase of the temperature at the inside surface, but in a decrease of the temperature at the outside surface of the conditioned space wall. The temperature variation for the unconditioned space wall is independent of the insulation level.

3.2 Heat flux distribution

Figure 7 presents the heat flux profiles at the conditioned space wall and floor inner surfaces for the six insulation configurations presented in Fig. 3. The heat flux profile for the case where the wall and floor are uninsulated is shown for a comparative analysis.

For all the insulation configurations, the wall/floor joint has higher heat flux than other wall and floor sections located away from the joint. This increase in heat flux at the wall/floor joint is a measure of the magnitude of the thermal bridging effects for each insulation configuration. As illustrated in Fig. 7, the insulation configuration that minimizes the thermal bridging effect of the wall/floor is that presented by case 4 and case 5 with insulation placed at the inner surface of both the wall and the floor. Indeed, the heat flow is almost one-dimensional along the entire building en-

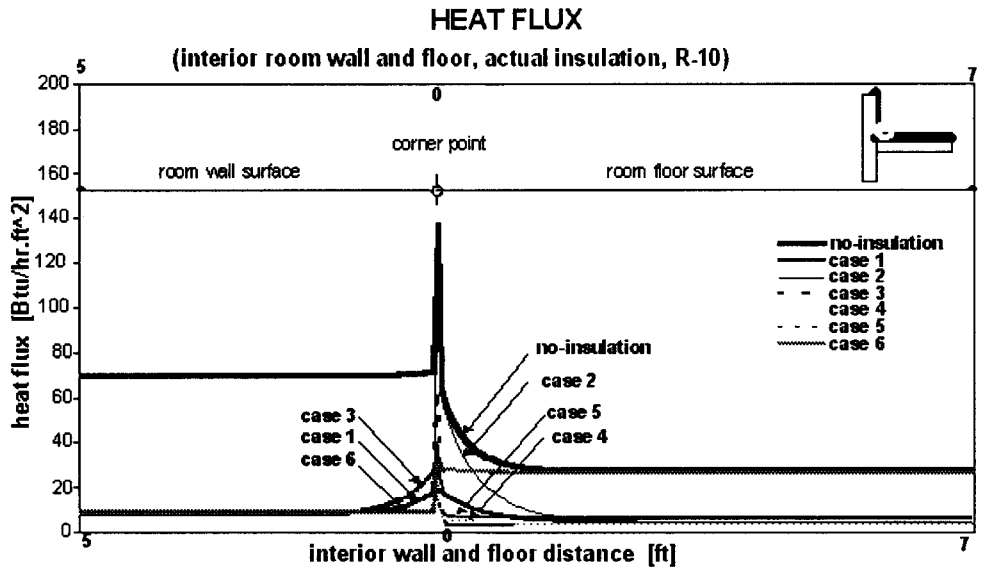

Fig. 7 Interior surface heat flux variation along the wall/floor surface (Conversion: [Btu/hr.ft^2]×3.15 =[W/m^2], [°F-32]×5/9=℃, 1 ft=0.3 m).

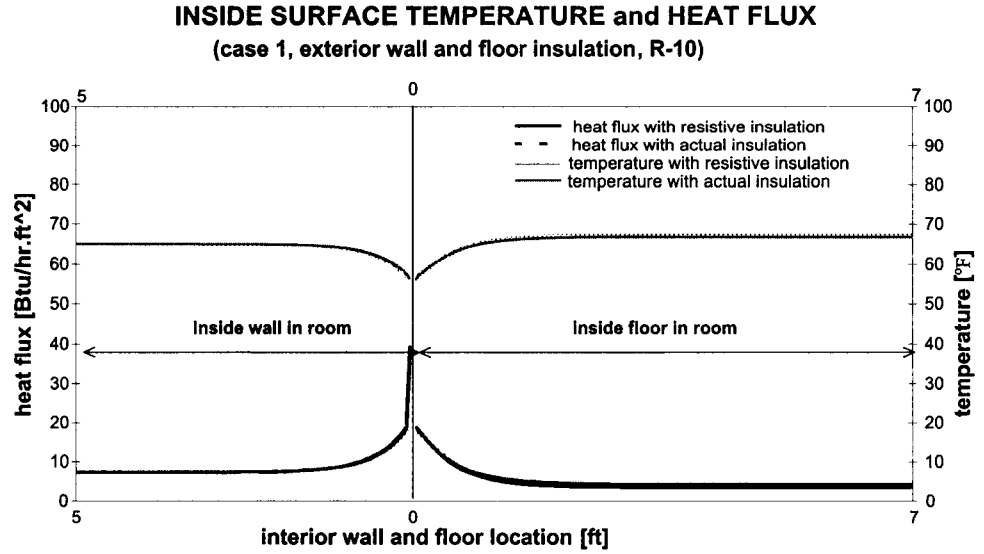

Fig. 8 Comparison between resistive and actual insulation modeling approaches (Conversion: [Btu/hr.ft^2]×3.15=[W/m^2], [°F-32]×5/9=℃, 1 ft=0.3 m).

velope interior surface for both cases 4 and 5.

Figure 8 shows the variation of the interior surface temperature and heat flux profile when the thermal insulation is placed at the outer surface of the wall (i.e. case 1 of Fig. 3). The insulation layer is modeled using the two approaches: (i) actual thickness is modeled, (ii) only a heat transfer coefficient is used to model the thermal insulation. As shown in Fig. 8, the two modeling approaches for the insulation provide almost the same surface temperature and heat flux profiles. Moreover, The

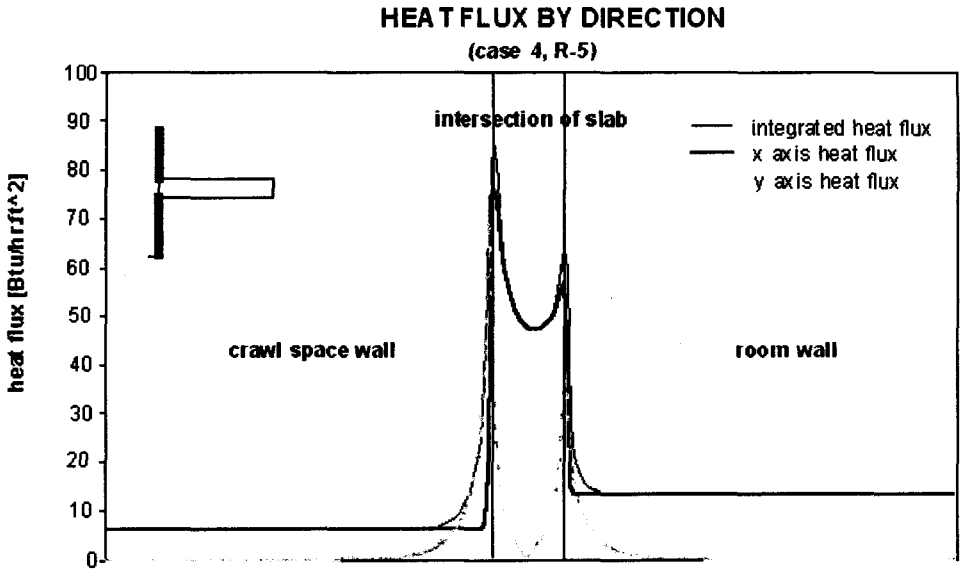

Fig. 9 Heat flux along the inner surface of the wall from the crawl space to the room (Conversion: [Btu/hr.ft^2]×3.15=[W/m^2], [°F-32]×5/9=℃, 1 ft=0.3 m).

temperature profile of Fig. 8 permits to assess the vulnerability of the wall and floor surfaces to any moisture condensation. For instance, Fig. 8 indicates that the inner surface temperature is below 58°F (14.4℃) at the wall/floor intersection. Therefore, whenever the indoor relative humidity is above 50%, moisture condensation can occur at the wall/floor intersection.

Figure 9 illustrates the two-dimensional character of the heat transfer along a vertical plane at the inner wall surface of both the conditioned and the unconditioned spaces. In particular, the heat flux along the x and the y directions are provided in Fig. 9 for case 4 insulation configuration with R-5 (1.03 m^2·℃/W) insulation layer. Through the selected vertical plane, the dominant heat flux occurs at the x-direction. However, a significant increase in both the x and y components of the heat flux occurs at the wall/floor joint. Specially, the y component of the heat flux becomes substantial only at the corners of the wall/floor joint indicating significant thermal bridging effects at these locations.

3.3 Total heat loss

Table 1 summarizes the total heat losses from the wall/floor intersection using the two insulation modeling approaches for cases 1 through 5. As indicated in Table 1, when the insulation layer is placed at the outer wall surface (i.e., cases 1 and 3 in Fig. 3), the thermal effect of the insulation can be modeled by simply modifying the surface heat transfer coefficient.

This modeling simplification allows an analytical solution of the same problem shown in Fig. 1 to be obtained using the ITPE technique as applied by Krarti[11] to analyze the thermal performance of building corners. However, this modeling simplification cannot be used when the insulation is placed at the inner wall surface as in cases 2, 4, and 5 of Fig. 3. Indeed, Table 1 indicates that modeling the insulation layer as a heat transfer coefficient can lead to 20% relative error in calculating the total heat loss for the insulation configuration of case 5.

Two methods are used to calculate the total heat losses: (i) one-dimensional approach using

Table 1 Comparison of resistive and actual insulation heat losses

		Heat loss 2-D [Btu/hr.ft] (W/m)		Total heat loss 2-D [Btu/hr.ft] (W/m)
		Wall (5 ft)	Floor (7 ft)	
CASE 1	Resistive	8.47 (8.81)	4.83 (5.02)	13.29 (13.83)
	Actual	8.38 (8.71)	5.42 (5.64)	13.80 (14.35)
	Percent of difference [%]	1.08	10.92	3.63
CASE 2	Resistive	7.30 (7.59)	8.23 (8.56)	15.53 (16.15)
	Actual	9.00 (9.36)	8.33 (8.66)	17.33 (18.02)
	Percent of difference [%]	18.93	1.15	10.39
CASE 3	Resistive	9.65 (10.03)	3.64 (3.78)	13.28 (13.81)
	Actual	9.16 (9.53)	3.82 (3.97)	12.98 (13.50)
	Percent of difference [%]	5.29	4.83	2.31
CASE 4	Resistive	7.34 (7.63)	3.80 (3.95)	11.13 (11.58)
	Actual	9.08 (9.44)	4.88 (5.07)	13.96 (14.51)
	Percent of difference [%]	19.18	22.17	20.23
CASE 5	Resistive	7.37 (7.66)	6.38 (6.64)	13.75 (14.30)
	Actual	9.13 (9.49)	7.62 (7.93)	16.75 (17.42)
	Percent of difference [%]	19.30	16.24	17.91

the classical thermal network technique, and (ii) the two-dimensional solution developed for this study. Table 2 summarizes the results of these calculations using three insulation levels R-5 (1.03 $m^2 \cdot ℃/W$), R-10 (2.05 $m^2 \cdot ℃/W$), and R-20 (4.10 $m^2 \cdot ℃/W$). The difference between the 1-D and 2-D heat losses indicates the magnitude of the thermal bridging effects for each

Table 2 Comparison of one and two-dimensional heat losses

		Heat loss 2-D [Btu/hr.ft] (W/m)	Heat loss 1-D [Btu/hr.ft] (W/m)	Difference Of 2-D and 1-D	Percent of difference [%]
No insulation		99.8 (103.7)	96.6 (100.5)	3.1 (3.3)	3.3
CASE 1	R - 5	22.1 (23.0)	19.6 (20.4)	2.5 (2.6)	12.7
	R - 10	13.3 (13.8)	10.9 (11.3)	2.4 (2.5)	21.9
	R - 20	8.2 (8.6)	5.8 (6.0)	2.5 (2.6)	42.8
CASE 2	R - 5	23.8 (24.7)	19.6 (20.4)	4.2 (4.4)	21.5
	R - 10	15.5 (16.1)	10.9 (11.3)	4.6 (4.8)	42.4
	R - 20	10.6 (11.0)	5.8 (6.0)	4.8 (5.0)	83.4
CASE 3	R - 5	21.8 (22.7)	19.6 (20.4)	2.2 (2.3)	11.3
	R - 10	13.3 (13.8)	10.9 (11.3)	2.4 (2.5)	21.8
	R - 20	8.4 (8.8)	5.8 (6.0)	2.6 (2.7)	45.7
CASE 4	R - 5	20.0 (20.8)	19.6 (20.4)	0.4 (0.4)	2.0
	R - 10	11.1 (11.6)	10.9 (11.3)	0.2 (0.2)	2.1
	R - 20	5.8 (6.1)	5.8 (6.0)	0.1 (0.1)	1.1
CASE 5	R - 5	23.7 (24.7)	23.5 (24.5)	0.2 (0.2)	0.9
	R - 10	13.8 (14.3)	13.6 (14.2)	0.1 (0.1)	0.8
	R - 20	7.4 (7.7)	7.4 (7.7)	0.0 (0.0)	0.2
CASE 6	R - 5	42.6 (44.3)	39.5 (41.1)	3.1 (3.2)	7.8
	R - 10	35.6 (37.0)	33.6 (34.9)	2.0 (2.1)	5.9
	R - 20	31.4 (32.7)	30.2 (31.4)	1.2 (1.2)	4.0

insulation configuration. Table 2 clearly shows that thermal bridging increases for cases 1, 2, and 3 but decreases for cases 4, 5, and 6 with the increase of the thermal resistance of the insulation. The best insulation configuration with minimal thermal bridging is case 4 with interior wall and floor insulation. Case 2 insulation configuration allows significant thermal bridging through the wall/floor joint and is therefore not recommended as an insulation scheme. It should be mentioned that case 6 provides the highest total heat loss from the wall/floor intersection since the floor separating the conditioned room from the unconditioned space is not insulated.

3.4 Transient results

Total heat loss is compared for all insulation configurations under transient conditions during one week representative of a cold climate. Figure 10 shows the results of the comparative analysis using Denver TMY weather data when R-10 (2.05 $m^2 \cdot ℃/W$) insulation layer is used for the configurations (case 1 through case 6). The results of the transient analysis confirm the basic findings of the steady-state analysis discussed in the previous section. Specifically, the heat loss from the conditioned space through the wall/floor intersection is minimized when the insulation is placed at the inner surface of both the wall and the floor (i.e., case 4 or 5) during the entire winter week considered in Fig. 10. Meanwhile, insulation configuration presented by case 6 (i.e., insulation placed only at the inner wall surface extending at the joint wall/floor) leads by the far to the worst thermal performance of the wall/floor intersection.

4. Conclusions

The thermal performance of wall/floor intersections is analyzed using an implicit finite difference solution. In particular, the analysis presented in this paper provides the temperature distribution within the building envelope, the heat flux profile along the interior wall and

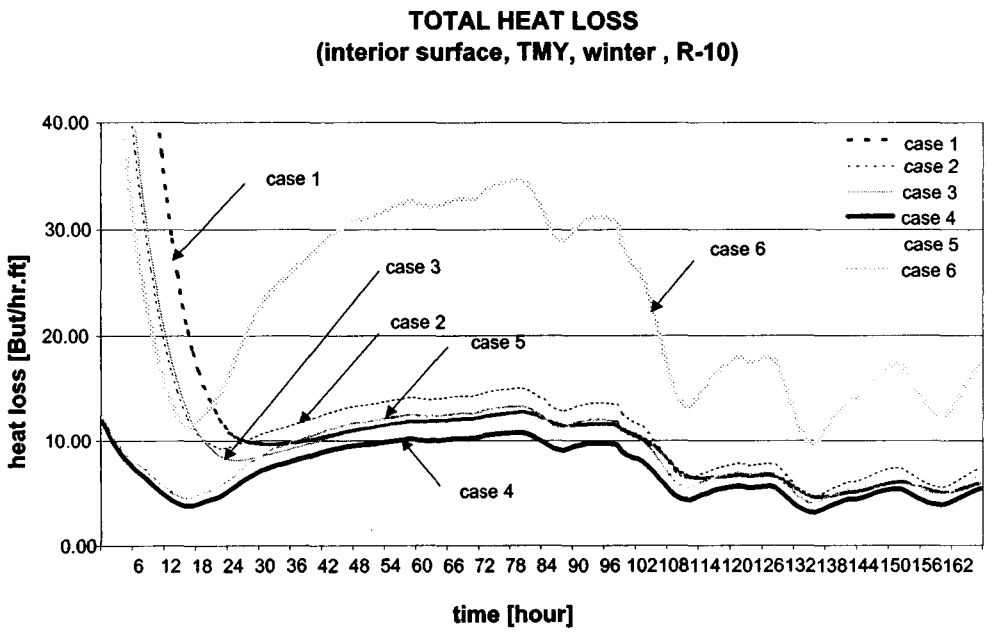

Fig. 10 Total heat loss profile during a winter week (Conversion: [Btu/hr.ft]×1.04=[W/m]).

floor surfaces, and the total heat losses/gains from the wall/floor intersection assembly. Based on the results of the analysis, it was found that by placing the thermal insulation at the inner surface of both the floor and the walls reduces significantly the thermal bridging effects. Moreover, it was found that the thermal insulation layer can be modeled by a simple heat transfer coefficient when the insulation is placed at the outer surface of the wall. This modeling simplification allows an analytical treatment of the heat transfer problem within a wall/floor intersection.

References

1. Carslaw, H. S. and Jaeger, J. C., 1959, Conduction of Heat in Solids, Clarendon Press, Oxford.
2. Langmuir, E. Q., Adams and Mekle, G. S., 1973, Flow of Heat Through Furnace Walls: The Shape Factors, pp. 55-84.
3. Letherman, K. M. and Sarkis, B. L., 1984, Building Environment, Vol. 19, p. 101.
4. Mathews, E. H., 1986, Building Environment, Vol. 21, p. 183.
5. Mao, G. and Johannesson, G., 1997, Dynamic calculation of thermal bridges, Energy and Building, Vol. 26, pp. 233-240.
6. Kim, K. S., Lee, D. B., Lee, J. H. and Park, H. S., 2004, A study on evaluation of insulation and condensation performance in corners of building envelope, Journal of the Architectural Institute of Korea Planning and Design, Vol. 16, No. 4. pp. 163-168.
7. Al-Sanea, S. A., 2003, Finite-volume thermal analysis of building roofs under two-dimensional periodic conditions, Building and Environment, Vol. 38, pp. 1039-1049.
8. Fukuyo, K., 2003, Heat flow visulization for thermal bridge problems, International Journal of Refrigeration, Vol. 26, pp. 614-617.
9. Pantankar, S., 1980, Numerical Heat Transfer and Fluid flow, New York, McGraw-Hill.
10. SIAM, 1993, LAPACK User's guide V2.0, Philadelphia, Pennsylvania.
11. Krarti, M., 1989, Steady-state heat transfer beneath partially insulated slab-on-grade floor, International Journal of Heat and Mass Transfer, Vol. 32 (5), pp. 961-969.